

# DESIGN STUDY OF SUPERCONDUCTING LINEAR ACCELERATOR FOR UNSTABLE ION BEAM IN RISF

Ji-Gwang Hwang, Chanmi Kim, Yumi Lee, Eun-San Kim\*

Kyungpook National University, Daegu, Korea

Hye-Jin Kim, Bong Hyuk Choi, Ilkyoung Shin, Hyojae Jang, Hyung Jin Kim, Dong-O Jeon

Institute for Basic Science, Daejeon, Korea

## Abstract

A post accelerator of RAON can accelerate unstable and stable ion beams up to 16.5 MeV/u for  $^{132}\text{Sn}^{16\sim 20+}$  and 16.0 MeV/u for  $^{58}\text{Ni}^{8+}$ , which has a ratio of mass to charge,  $A/q$ , of 8.3. The unstable ion beam such as  $^{132}\text{Sn}^{20+}$  produced by an ISOL system has the large transverse and longitudinal emittances. Hence an acceptance and envelope of the post accelerator should be optimized for safety operation. The beams accelerated by the post accelerator were transported by a post-to-driver transport (P2DT) line which consists of a charge stripper, two charge selection sections. Then the beams are accelerated up to 200 MeV/u in the high energy linac. In this paper, we will show a criteria for the design of the post accelerator and results of beam tracking simulation from the exit of the ISOL system to the end of the high energy linac.

## INTRODUCTION

The linear accelerator with a superconducting technology for heavy ion beams named as a RAON (Rare isotope Accelerator Of Newness) was launched to examine the numerous facets of basic science, such as nuclear physics, astrophysics, atomic physics, life science, medicine and material science [1]. The unstable ion beams was produced by a ISOL based ion source and it was accelerated up to 16.5 MeV/u for  $^{132}\text{Sn}$  ion beams and 16.0 MeV/u for  $^{58}\text{Ni}$  ion beams with a high repetition rate of 81.25 MHz. The elec-

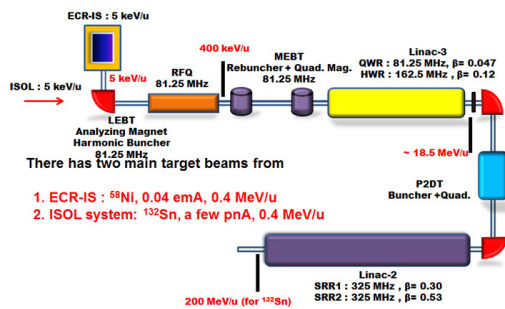


Figure 1: The schematic layout of the post linac.

trons of the ion beam are stripped by the charge stripper to increase the acceleration efficiency at the high energy linear accelerator and it is transported to high energy lin-

ear accelerator through the post-to-driver transport (P2DT) beam line. The schematic layout is shown in Fig. 1.

## TRACKING SIMULATION OF THE POST LINAC FOR $^{132}\text{SN}$ ION BEAM

In order to demonstrate the beam quality in the post linac, the particle tracking simulation from the low-energy beam transport (LEBT) line to the end of the high energy linac was performed with 500k macro-particles. The  $^{132}\text{Sn}^{20+}$  beam was produced by the ISOL system with the energy of 5 keV/u and it was accelerated up to 400 keV/u by the RFQ accelerator. The initial particle coordinates of the macro-particles were obtained using the tracking simulation from the LEBT to MEFT by the codes TRACK and PARMTEQ. The distribution at the entrance of the post linac is shown in Fig. 2.

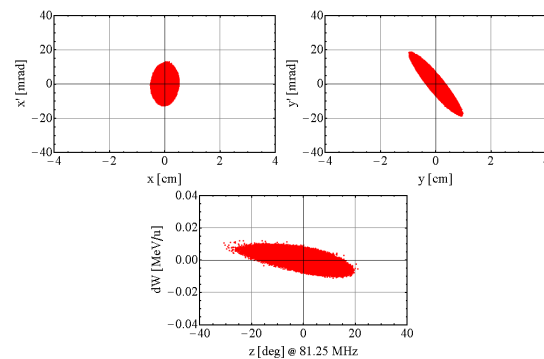


Figure 2: The particle distributions of  $^{132}\text{Sn}^{20+}$  on 6D phase space at the entrance of the post linac.

The beam energy, rms horizontal and vertical emittances, and longitudinal emittance are 0.405 MeV/u, 0.282 mm-mrad, 0.287 mm-mrad and 0.464 keV/u-ns, respectively.

In order to suppress many instabilities which can cause the particle loss in the linac such as the envelope instability, parametric resonance and the space charge effect, the zero current phase advances,  $\sigma_0$ , is set to lower than  $90^\circ$  [2]. A low phase advance per period, and consequently a smooth focusing, has some costs in terms of beam dimensions, but guarantees the stability of envelope oscillations [3]. The ratio between the zero current transverse and longitudinal phase advance,  $\phi_z/\phi_x$  and  $\phi_z/\phi_y$ , were also almost kept between 1.0 and 1.5 except the matching section to vanish the effect of the parametric resonance [2]. Figure 3 shows

\* eskim1@knu.ac.kr

the rms beam envelope, and rms transverse and longitudinal emittances along the post linac. It was calculated by the multi-particle tracking simulation using code TRACK, which can compute multi-particle simulation of multiple component ion beams in 6D phase space [4].

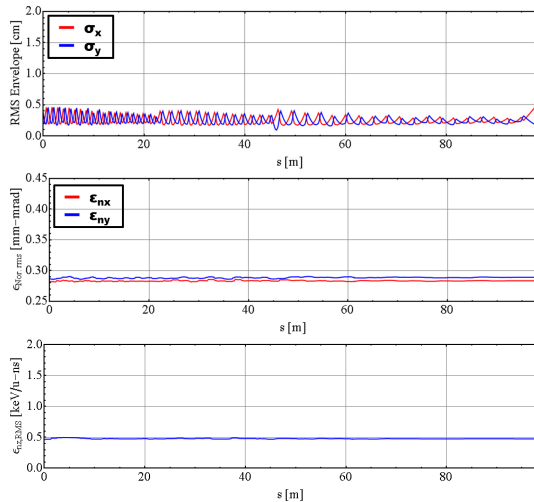


Figure 3: The envelopes of the beam size (top), transverse emittance (middle) and longitudinal emittance (bottom) in the post linac.

Since the rms transverse emittance of the  $^{132}\text{Sn}$  provided from the ISOL system is about 0.3 mm-mrad, the rms envelope in the linac is larger than 4 mm even through the beam size was minimized. The growths of the transverse and longitudinal emittance are ignorable. To minimize the emittance growth due to the effect of angular straggling at the charge stripper, the beam ellipse in the transverse phase space was controlled to reach the stripper with an upright ellipse [5]. The particle distributions on the 6D phase space at the end of the post linac are shown in Fig 4.

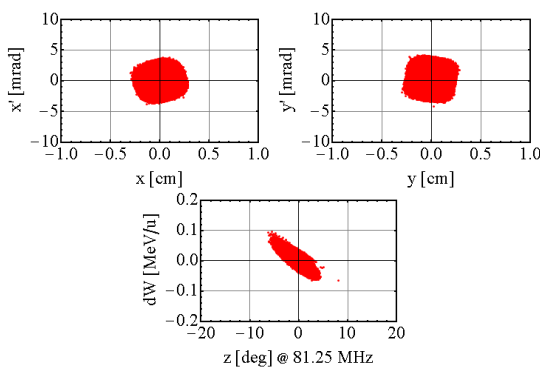


Figure 4: The particle distributions of  $^{132}\text{Sn}^{20+}$  on 6D phase space at the exit of the post linac.

The beam energy, rms horizontal and vertical emittances, and longitudinal emittance are 16.53 MeV/u, 0.284 mm-mrad, 0.289 mm-mrad and 0.475 keV/u-ns, respectively.

ISBN 978-3-95450-142-7

## TRACKING SIMULATION OF THE POST-TO-DRIVER TRANSPORT LINE

The post-to-driver transport (P2DT) line which consists of two  $90^\circ$  bending section for the selection of the charge state of the desired beam and telescope section for the beam transportation of long distance. It also included a several beam diagnosis and cavities for longitudinal bunching. The layout of the P2DT beam line is shown in Fig. 5

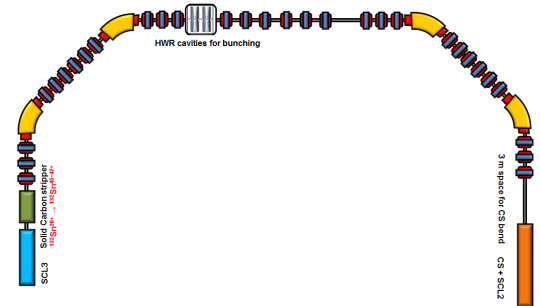


Figure 5: The layout of the P2DT beam line.

Since the dispersion in the first  $90^\circ$  bending section is required to eliminate the undesired beams, the trajectories on the horizontal plane are different with each charge state of the beam. It causes the time delay between the charge states. To compensate for this effect, the cavities for the longitudinal bunching is installed at the exit of the first  $90^\circ$  bending section. Figure 6 shows the rms beam envelope, and rms transverse and longitudinal emittances along the P2DT line.

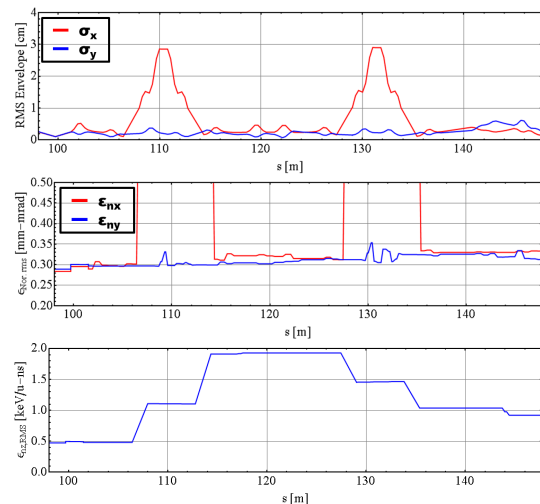


Figure 6: The envelopes of the beam size (top), transverse emittance (middle) and longitudinal emittance (bottom) in the P2DT line.

The growth of the transverse emittance due to the angular straggling effect in the stripper was well compensated and the longitudinal emittance was well controlled by two cavities. The particle distributions at the exit of the P2DT beam line are shown in Fig. 7.

02 Proton and Ion Accelerators and Applications

2B Ion Linac Projects

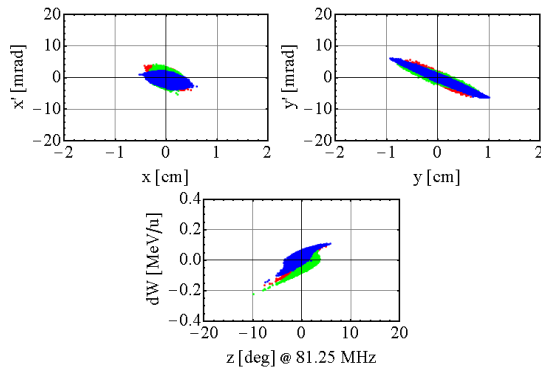


Figure 7: The particle distributions of  $^{132}\text{Sn}^{45+}$  (green),  $^{132}\text{Sn}^{46+}$  (red) and  $^{132}\text{Sn}^{47}$  (blue) on 6D phase space at the exit of the P2DT line.

The beam energy, rms horizontal and vertical emittances, and longitudinal emittance are 16.54 MeV/u, 0.333 mm-mrad, 0.313 mm-mrad and 0.921 keV/u-ns, respectively.

### TRACKING SIMULATION OF HIGH ENERGY LINAC

The high energy linear accelerator of the RAON, which consists of two-type single spoke cavities, accelerate the  $^{132}\text{Sn}$  ion beam up to 200 MeV/u to perform the experiments for exotic nuclear reactions induced by the unstable nuclei and the structures of unstable nuclei. In order to suppress many instabilities, the zero current phase advances,  $\sigma_0$ , is set to lower than  $90^\circ$ . The rms beam envelope, and rms transverse and longitudinal emittances along the high energy linac are shown in Fig. 8.

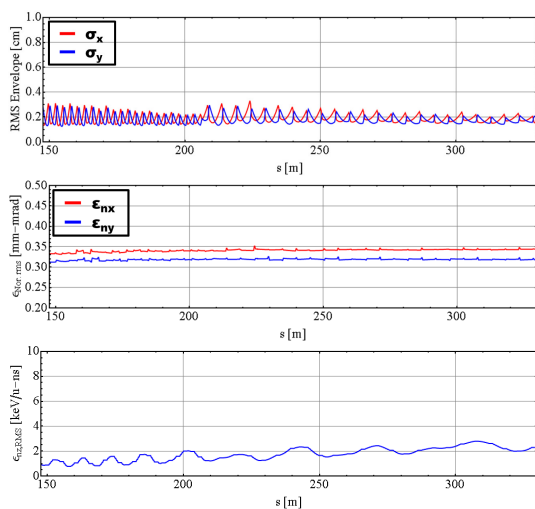


Figure 8: The envelopes of the beam size(top), transverse emittance (middle) and longitudinal emittance (bottom) in the high energy linac.

The rms envelope in the high energy linac was kept less than 4 mm for vanishing the beam loss and the severe growth of the transverse and longitudinal emittances is not

observed in the high energy linac. The beam energy, rms horizontal and vertical emittances, and longitudinal emittance are 212.66 MeV/u, 0.344 mm-mrad, 0.318 mm-mrad and 2.29 keV/u-ns, respectively. The particle distributions on the 6D phase space at the end of the high energy linac are shown in Fig 9.

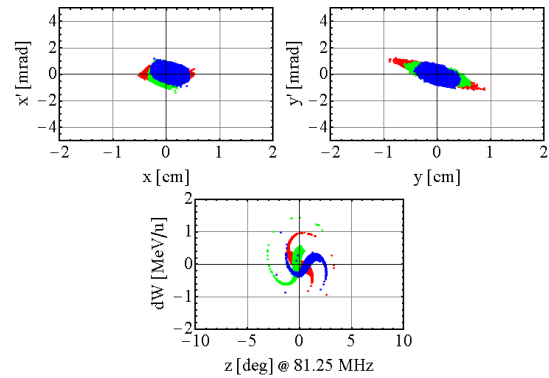


Figure 9: The particle distributions of  $^{132}\text{Sn}^{45+}$  (green),  $^{132}\text{Sn}^{46+}$  (red) and  $^{132}\text{Sn}^{47}$  (blue) on 6D phase space at the exit of the high energy linac.

### CONCLUSION

The particle tracking simulation from the LEBT to high energy linac for demonstrating the performance of the linac of RAON for unstable nuclei, which is used to provide the high energy unstable ion beams produced by the ISOL system, was performed. The phase advance in the designed linac was kept to avoid the envelope instability and the space charge effect. The ratio of phase advance between the transverse and longitudinal was controlled between 1 and 1.5 to avoid the parametric resonance. The P2DT beam line was designed for selection of the desired beam and transportation of the beam to the high energy linac, and the position and number of cavities for bunching were optimized. Based on the multi-particle tracking simulation, the transverse emittance growth from the ISOL system to the high energy linac is less than 22 %. It is mainly caused in the P2DT beam line.

### REFERENCES

- [1] <http://www.ibs.re.kr>.
- [2] Ji-Gwang Hwang, et al., Proceedings of IPAC2014, Dresden, Germany, THPME148 (2014).
- [3] A. Pisent, INSTABILITIES IN LINEAR ACCELERATORS, CERN-2005-004 p.198.
- [4] P. N. Ostromov and K. W. Shepard, Phys. Rev. ST. Accel. Beams, **11**, 030101 (2001).
- [5] Ji-Gwang Hwang, et al., "Minimization of the emittance growth of multi-charge particle beams in the charge stripping section of RAON", *Nucl. Instrum. Methods A*, to be published [Online]. Available: <http://www.sciencedirect.com/science/article/pii/S0168900214009383>, (2014).